Multinucleon transfer processes in the ^{197}Au+^{130}Te reaction studied with a high-resolution kinematic coincidence

F. Galtarossa[1,2], L. Corradi[1] and S. Szilner[3], E. Fioretto[1], G. Pollarolo[4], T. Mijatović[3], D. Montanari[5], D. Ackermann[6], D. Bourgin[7], S. Courtin[7], G. Fruet[7], A. Goasduff[1], J. Grebosz[8], F. Haas[7], D. Jelavić Malenica[3], S. C. Jeong[9], H. M. Jia[10], P. R. John[5], D. Mengoni[5], M. Milin[11], G. Montagnoli[5], F. Scarlassara[5], N. Skukan[3], N. Soić[3], A. M. Stefanini[1], E. Strano[5], V. Tokić[3], C. A. Ur[12], J. J. Valiente-Dobón[1], Y. X. Watanabe[9]

[1]Istituto Nazionale di Fisica Nucleare, Laboratori Nazionali di Legnaro, Legnaro, Italy
[2]Dipartimento di Fisica e Scienze della Terra, Università di Ferrara, Ferrara, Italy
[3]Ruđer Bošković Institute Zagreb, Croatia
[4]Dipartimento di Fisica, Università di Torino, and Istituto Nazionale di Fisica Nucleare, Torino, Italy
[5]Dipartimento di Fisica, Università di Padova, and Istituto Nazionale di Fisica Nucleare, Padova, Italy
[6]GANIL, CEA/DSM-CNRS/IN2P3, Boulevard Henri Becquerel, Caen, France
[7]Institut Pluridisciplinaire Hubert Curien, CNRS-IN2P3, Université de Strasbourg, Strasbourg, France
[8]The Henryk Niewodniczanski Institute of Nuclear Physics, Krakow, Poland
[9]Institute of Particle and Nuclear Studies, High Energy Accelerator Research Organization (KEK), Tsukuba, Ibaraki, Japan
[10]China Institute of Atomic Energy, Bejing, China
[11]Department of Physics, Faculty of Science, University of Zagreb, Zagreb, Croatia
[12] Horia Hulubei National Institute of Physics and Nuclear Engineering, Bucharest, Romania

Abstract

Multinucleon transfer processes in the ^{197}Au+^{130}Te at E_{lab}=1.07 GeV system were studied with the PRISMA magnetic spectrometer in coincidence with an ancillary particle detector. For neutron transfer channels we extracted total cross sections and compared them with calculations performed with the GRAZING code. We associated to each light fragment identified in PRISMA the corresponding mass distribution of the heavy partner and, through the comparison with Monte Carlo simulations, we could infer about the role of neutron evaporation in multinucleon transfer for the population of neutron-rich heavy nuclei.

1 Introduction

The production of neutron-rich nuclei close to the N = 126 shell closure is fundamental to investigate different physical scenarios, ranging from shape coexistence phenomena in neutron-rich Pt-Os isotopes [1] to the path chosen by the r-process to synthesize the heaviest elements [2]. Accessing this region is not an easy task due to the lack of suitable beam-target combinations. Fusion reactions with stable beams and fission yield quite low cross sections and the beam intensities from radioactive beam facilities are not sufficient to perform detailed nuclear structure studies.

Nuclear reaction models [3,4] predict large primary cross sections employing multinucleon transfer (MNT) reactions. One has to keep in mind that at energies close to the Coulomb barrier, multinucleon transfer reactions are mainly governed by optimum Q-value considerations and nuclear form factors [5,6]. For this reason with stable projectiles and targets the main open channels are neutron pick-up and proton stripping from the light partner, while the inverse path can be accessed if neutron-rich projectile and targets are employed, as was recently shown in [7].

Recent experiments have shown that MNT reactions are in fact a suitable and complementary mechanism to fragmentation reactions at relativistic energies for the production of neutron-rich nuclei in the Pb region. In Ref. [8] the products of the fragmentation of ^{208}Pb at 1 A GeV on a Be target were identified in charge Z and mass A with good resolution, due to their high energy. The production cross sections decrease rapidly moving to the neutron-rich side but the reaction products are strongly forward focused and considerable yields can be obtained. In Ref. [9] MNT reactions in the ^{136}Xe+^{198}Pt system at $E_{lab} \sim 8$ A MeV were studied with the magnetic spectrometer VAMOS++ coupled to the EXOGAM γ array. In this case the direct identification in Z and A of the heavy partner was extremely challenging and the production cross sections for the Pt-like ions could only be reconstructed in a complex iterative way from the measured yields and total kinetic energy loss (TKEL) distributions of the primary fragments. These cross sections turned out to be higher compared to those obtained in the fragmentation case, but the authors stressed that neutron-rich heavy nuclei are populated in transfer reactions involving low excitation energies, thus increasing the probability for the primary heavy partner to survive the effect of secondary processes, like nucleon evaporation or fission.

To better understand the effect of such competitive processes we performed an experiment at the INFN Laboratori Nazionali of Legnaro (LNL) to study MNT reactions at near-barrier energies in the ^{197}Au+^{130}Te (E_{lab} = 1.07 GeV). We chose the most neutron-rich Te stable isotope as a target to open the proton and neutron transfer channels leading to neutron-rich heavy partners. We employed a novel experimental method which aims at the simultaneous detection of light and heavy transfer products where one of the reaction partners (the light one) is identified with high A and Z resolution. This allows to correlate the masses of the two reaction partners and follow the behaviour of the heavy partner after the transfer process. The choice of the inverse kinematics allows to have enough kinetic energy of the recoils for their detection though maintaining a low bombarding energy.

2 The experiment and the analysis

For the experiment we used a 1.5-pnA ^{197}Au beam delivered by the PIAVE positive-ion injector followed by the ALPI post accelerator of LNL, impinging onto a 200 μg/cm^2 (2-mm strip) ^{130}Te target with a purity of 99.6%. The layout of the experimental set-up is depicted in Figure 1.

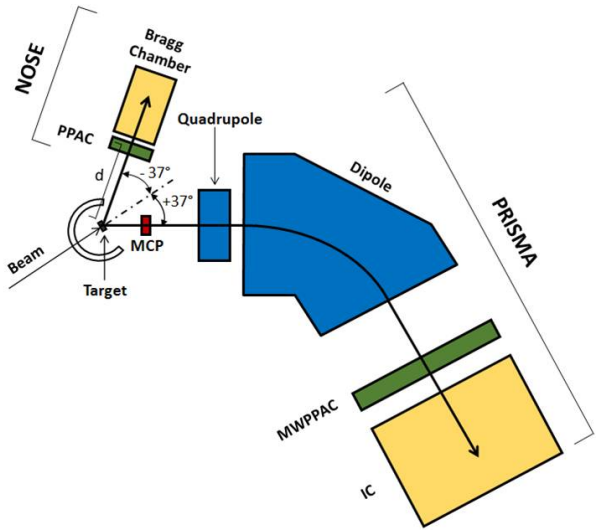

Fig. 1: Layout of the set-up used in the study of the ^{197}Au+^{130}Te reaction, with the PRISMA spectrometer set in coincidence with the NOSE detector. Bragg chamber: axial field ionization chamber; PPAC: multiwire parallel-plate avalanche counter of NOSE; MCP: micro-channel plate detector; MWPPAC: parallel-plate detector of multiwire type; IC: ionization chamber of PRISMA.

The PRISMA magnetic spectrometer [10] was employed for the detection of Te-like ions. The heavy partner was identified in NOSE [11], the ancillary detector coupled to PRISMA, composed of a MWPPAC followed by an axial ionization chamber (Bragg chamber). PRISMA and NOSE were placed at the symmetric angles of $\pm$ 37° for kinematic reasons.

Figure 2 shows the quality of the Z identification in the ionization chambers of the two detectors. In PRISMA (left) the nuclear charge is measured with the E-ΔE technique. The inset shows that the Z resolution (ΔZ/Z $\sim$ 1/65) allows to distinguish several proton transfer channels. The cross sections for these channels are about one order of magnitude less than for neutron transfer, due to the chosen low bombarding energy. For this reason in this work we will focus on pure neutron transfer channels. In NOSE the nuclear charge is measured according to the principle of Bragg Curve Spectroscopy [12]. In this case it is not possible to distinguish proton transfer channels for the heavy partner but a clear separation between Te-like and Au-like events is visible.

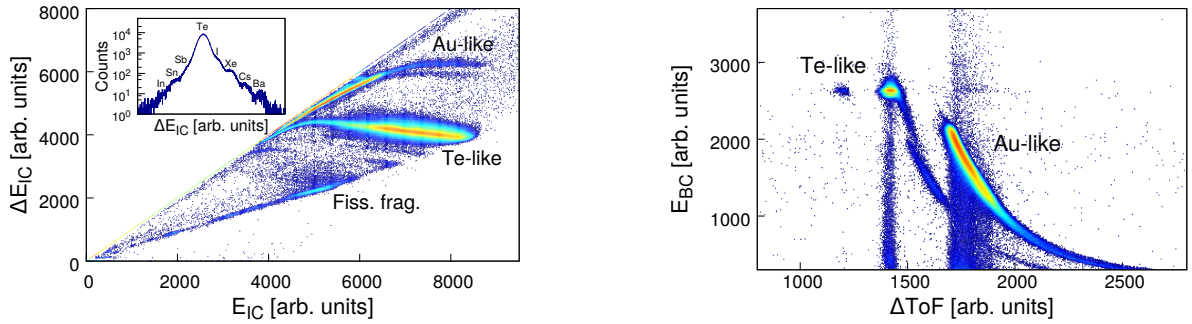

Fig. 2: (Left) Matrix of ΔE_{IC} versus energy E_{IC} of the PRISMA ionization chamber for the ^{197}Au+^{130}Te reaction at E_{lab}=1.07 GeV and θ_{lab}=37°. Besides the Te-like and Au-like ions, those corresponding to fission events, which are not stopped in the IC, are labeled. Inset: Z distributions of the reaction products in the Te region. (Right) Two-dimensional matrix of total energy measured with the Bragg chamber (E_{BC}) vs the time-of-flight between the MCP of PRISMA and the PPAC of NOSE (ΔToF). The clearly separated Te-like and Au-like events are labeled.

In PRISMA the mass identification is performed on an event-by-event basis through the reconstruction of the ions trajectory inside the magnetic elements of the spectrometer, from the measurement of the entrance and exit position of the ions on a MCP detector and a MWPPAC detector, respectively. Figure 3 (left) shows the resulting mass spectrum for Te ions. The mass resolution is ΔA/A $\sim$ 1/240. Transfer channels down to the stripping of 6 neutrons are visible. These are the channels that lead to the population of neutron-rich Au ions.

The experimental yields could be compared with theoretical calculations performed with the GRAZING code [13, 14] that implements a model of the collision that is predominantly binary. The model calculates the evolution of the reaction by taking into account, besides the relative motion variables, the intrinsic degrees of freedom of projectile and target. These are the surface degrees of freedom and the one-nucleon transfer channels. The relative motion of the system is calculated in a nuclear plus Coulomb field. The exchange of many nucleons proceeds via a multi-step mechanism of single nucleons.

To compare calculations and experimental data we normalized the measured yields to the ^{129}Te, keeping the same normalization constant for all the other transfer channels. This is made possible by the fact that for neutron transfer the angular distributions have similar shapes and the acceptance of PRISMA selects the same fraction of events for the different transfer channels. The comparison clearly shows that neutron evaporation must be taken into account to reproduce the experimental cross sections.

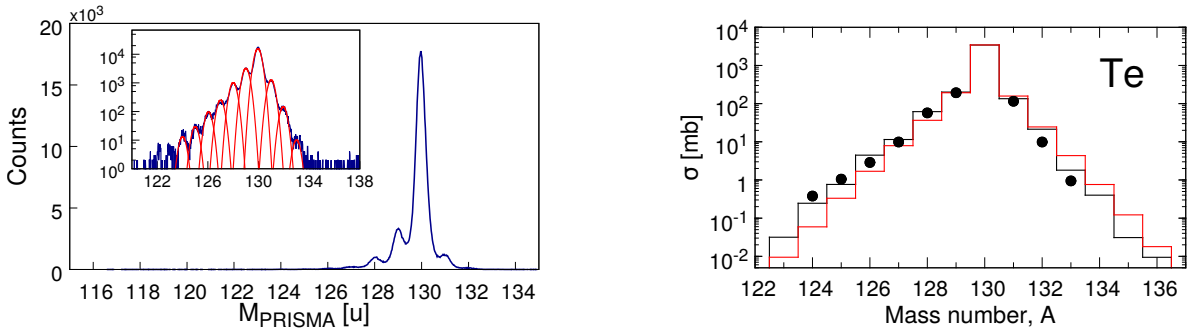

Fig. 3: (Left) Mass distribution for the Te isotopes obtained after ion trajectory reconstruction in PRISMA. The inset shows the distribution in logarithmic scale with the multigaussian fit used to evaluate the yields of neutron transfer channels. (Right) Total experimental cross sections of Te isotopes (points) and GRAZING calculations with (black histogram) and without (red histogram) taking into account the effect of evaporation. Errors are only statistical and are within symbols.

2.1 Mass-mass correlation and Monte Carlo simulations

Indicating the collision as $A + a \rightarrow B + b$ the mass M_B of the heavy partner can be determined from the measured scattering angles, θ_b in PRISMA and θ_B in NOSE, and of the time-of-flight τ_B taken by the heavy partner to cover the distance d $\sim$ 90 cm from the target to the PPAC of NOSE. We call p_A the momentum of the beam in the laboratory frame, we assume a binary character of the reaction and impose momentum conservation, finally obtaining:

$$M_B = \frac{p_A}{d} \frac{sin\theta_b}{sin(\theta_b + \theta_B)} \tau_B \tag{1}$$

The mass resolution strongly depends on the resolution on τ_B and is only slightly affected by the angular resolution. The obtained value is ΔA/A $\sim$ 1/40, which means $\sim$ 5 mass units for the Au-like mass distribution. The kinematic coincidence allows to construct a mass-mass correlation matrix, as shown in Fig. 4, where the total mass distribution of the heavy partner results to be divided in well-separated bands in correspondence of the coincident light fragment identified in PRISMA.

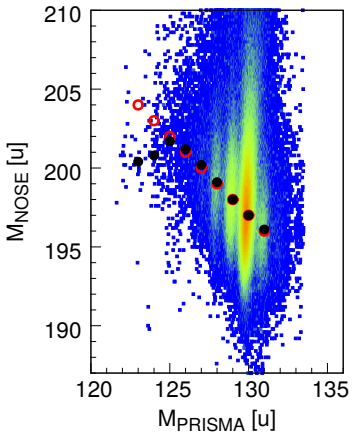

Fig. 4: Mass-mass correlation matrix of Te isotopes detected in PRISMA and the heavy partner detected in coincidence with NOSE. The red circles indicate the centroids of the correlated masses of the primary neutron transfer channels, the black dots indicate the experimental centroids as derived from the fits of their projections.

One can notice that after the transfer of $\sim$ 3-4 neutrons the centroids of the experimental distributions (full black circles) begin to deviate from the expected trend of the primary centroids (empty red circles). The shift between primary and secondary centroids is an effect of the onset of neutron evaporation.

More quantitative information can be extracted by comparing the mass distributions of the heavy partner associated to each Te isotope, which can be obtained by projecting the mass-mass correlation matrix on the y axis for each transfer channel, with Monte Carlo (MC) simulations. The inputs to the MC simulation are the relevant experimental observables (measured cross sections, TKEL distributions, experimental resolution). Then, starting from a given event as recorded by PRISMA and assuming a binary character of the reaction, we can follow the behavior of the heavy partner after the reaction. From the measured TKEL ditributions we can assign an excitation energy to the heavy partner assuming, in first approximation, an equal sharing of the energy between the two fragments. More details can be found in Ref. [15].

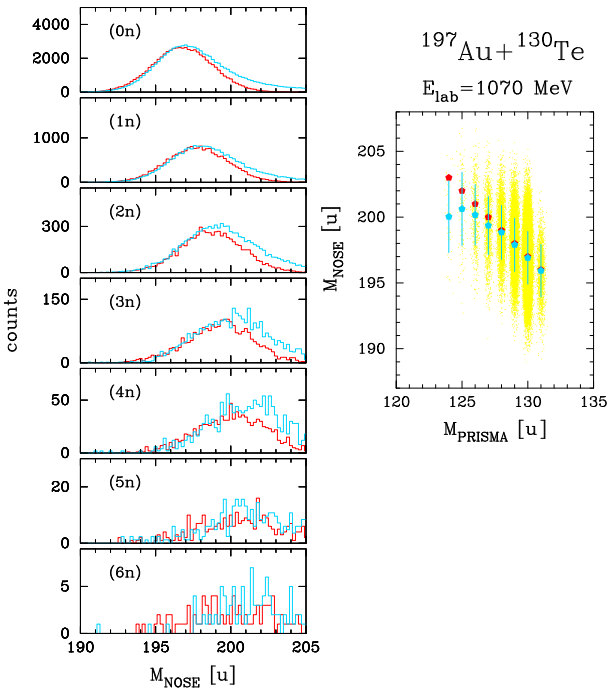

Fig. 5: (Right) Simulated mass-mass correlation matrix. The points are the centroids of the primary (red) and actual (blue) Au isotope distributions. The blue bars represent the standard deviations. (Left) Comparison between the simulated (red) and experimental (blue) mass distributions obtained from the projection of the corresponding mass-mass matrix. The label in each frame indicates the number of neutrons stripped from ^{130}Te.

The comparison between simulated and experimental Au mass distributions is shown in Fig. 5. Neutron evaporation, besides shifting the secondary centroids with respect to the primary ones, shows up as an increase of the width of the mass distributions as more neutrons are transferred.

3 Conclusions

In this contribution we presented our method to measure the effect of neutron evaporation on the heavy partner in the multinucleon transfer reaction ^{197}Au+^{130}Te at E_{lab} = 1.07 GeV, focusing on pure neutron transfer channels. We identified the light partner in A, Z and Q value in PRISMA and determined the mass of the heavy partner in NOSE from momentum conservation in a binary collision. We compared the extracted cross sections for the light partner with the predictions of GRAZING and obtained an

overall good agreement. We constructed a mass-mass correlation matrix and, through the comparison with Monte Carlo simulation, we could evidence the role of evaporation in multinucleon transfer.

References

[1] P. R. John, *et al.*, Phys. Rev. C **90**, 021301(R) (2014); Phys. Rev. C **95** 064321 (2017).

[2] H. Grawe, *et al.*, Rep. Prog. Phys. **70**, 1525 (2007),

[3] C. H. Dasso, G. Pollarolo, and A. Winther, Phys. Rev. Lett. **73**, 1907 (1994).

[4] V. Zagrebaev and W. Greiner, Phys. Rev. Lett. **101**, 122701 (2008).

[5] R. A. Broglia and A. Winther, *Heavy Ion Reactions* (Addison- Wesley, Redwood City CA, 1991).

[6] L. Corradi, G. Pollarolo, and S. Szilner, J. Phys. G: Nucl. Part. Phys. **36**, 113101 (2009).

[7] T. Mijatović, *et al.*, Phys. Rev. C **94**, 064616 (2016).

[8] T. Kurtukian-Nieto, *et al.*, Phys. Rev. C **89**, 024616 (2014).

[9] Y. X. Watanabe, *et al.*, Phys. Rev. Lett. **115**, 172503 (2015).

[10] S. Szilner, *et al.*, Phys. Rev. C **76**, 024604 (2007).

[11] E. Fioretto, *et al.*, Nucl. Instr. and Meth. in Phys. Res. A **899** (2018) 73-79.

[12] C. Gruhn, *et al.*, Nucl. Instr. and Meth. in Phys. Res. **196** (1982).

[13] A. Winther, Nucl. Phys. A **572**, 191 (1994); Nucl. Phys. A **594**, 203 (1995).

[14] Program GRAZING [http:/www.to.infn.it/∼nanni/grazing]

[15] F. Galtarossa, *et al.*, Phys. Rev. C **97**, 054606 (2018).